POSTER NOTE

Enhanced Structural Resolution in HRPF: Integrating AutoFox® Labeling with Astral Zoom DIA for Comprehensive Small Molecule Binding Site Characterization

Emily Chea[1], Chuck Mobley[1], David Tab[2], Yuqi Shi[3], Weijing Liu[3], and Scot Weinberger[1]

1. *GenNext Technologies, Inc.*
2. *University Medical Center Groningen*
3. *Thermo Fisher Scientific*

KEY TAKEAWAYS

- **Increase Residues Detected**
- **Small Molecule Binding Detected**
- **Allosteric Effects Mapped**
- **High Resolution Structural Biology**

Structural Biology the Easy Way

Computational biology and artificial intelligence (AI) are revolutionizing therapeutic development by rapidly generating structural and interaction models for biotherapeutics and small molecules. Despite significant investments and advances in AI, empirical validation remains crucial due to frequent predictive failures in dynamic protein conformations, allosteric changes, and intrinsically disordered regions. Conventional validation techniques (NMR, X-ray crystallography, cryo-EM) are costly, slow, and require extensive sample quantities, hindering timely therapeutic advancements.

GenNext's AutoFox Protein Footprinting System overcomes these challenges, providing rapid empirical validation and high-resolution insights into protein structure and interactions at significantly lower costs and sample requirements.

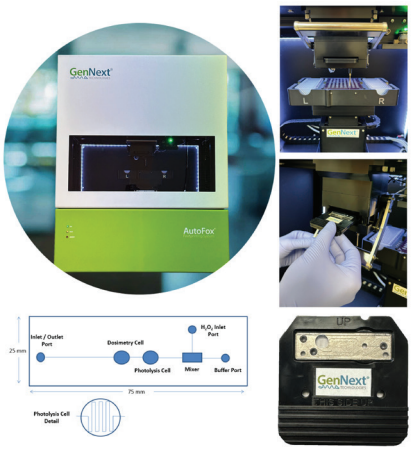

Figure 1: Automated & Reproducible Labeling. *HRPF labeling is performed in an automated fashion using a 96-well plate in the AutoFox System. Sample delivery, reagent mixing, and flashing are performed through a microfluidic chip designed to maximize irradiated volume. Samples are quenched in an adjacent well prior to LC-MS/MS analysis.*

Fully Automated HRPF Labeling

The AutoFox System uses a proprietary flash oxidation lamp to generate hydroxyl radicals (•OH), rapidly modifying solvent-exposed amino acid side chains. These covalent modifications provide a direct, quantitative measure of solvent accessibility and conformational dynamics, offering critical insights into protein higher order structure. With fully automated and reproducible labeling, the AutoFox enables precise spatial mapping of protein folding, surface topology, and interaction interfaces—supporting high-confidence analysis of protein–protein and protein–ligand interactions.

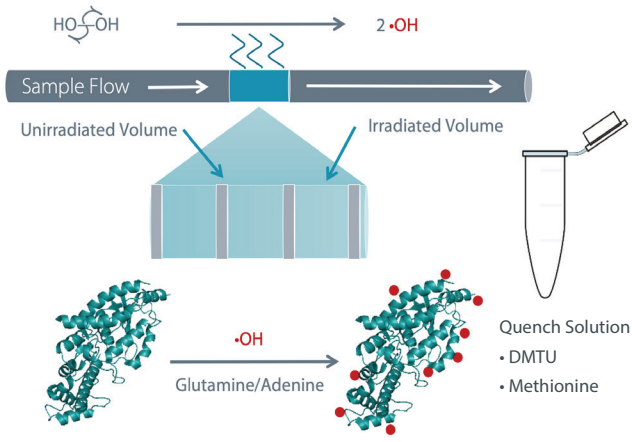

Figure 2: Schematic of the AutoFox Footprinting Method. *With this method, protein is mixed with hydrogen peroxide and flowed passed a flash lamp which photolyzes the hydrogen peroxide into two •OH and modifies solvent exposed amino acids. Following labeling, the sample is deposited into a quench solution of DMTU and methionine.*

Protein Footprinting with the AutoFox System

Precision. Reproducibility. Confidence.

The AutoFox System delivers highly reproducible and accurate Hydroxyl Radical Protein Footprinting (HRPF) data—empowering confident decision-making in biopharmaceutical discovery and development.

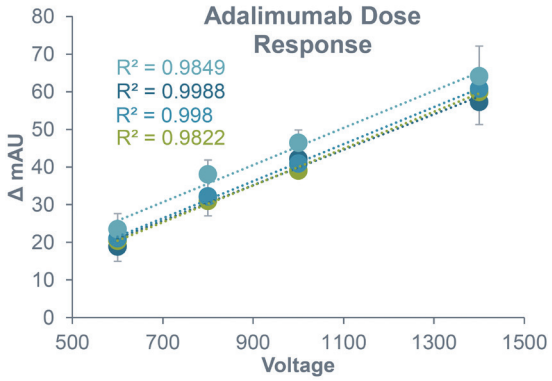

Figure 3: High Reproducibility of Protein Dose Response Curves Using the AutoFox System. *Dose response curves generated by the AutoFox System exhibit strong linear correlation ($R^2 > 0.98$) between hydroxyl radical concentration (Δ mAU) and the voltages applied (V) with excellent relative standard deviations (RSDs) of ~1–11% across three technical replicates. Four independent biological replicates were conducted on different days, using separate chips and operators, demonstrating the system's robust day-to-day reproducibility.*

Experimental Workflow

HRPF-LCMS structural comparison of KRAS G12C ± Sotorasib using DDA and DIA acquisition strategies

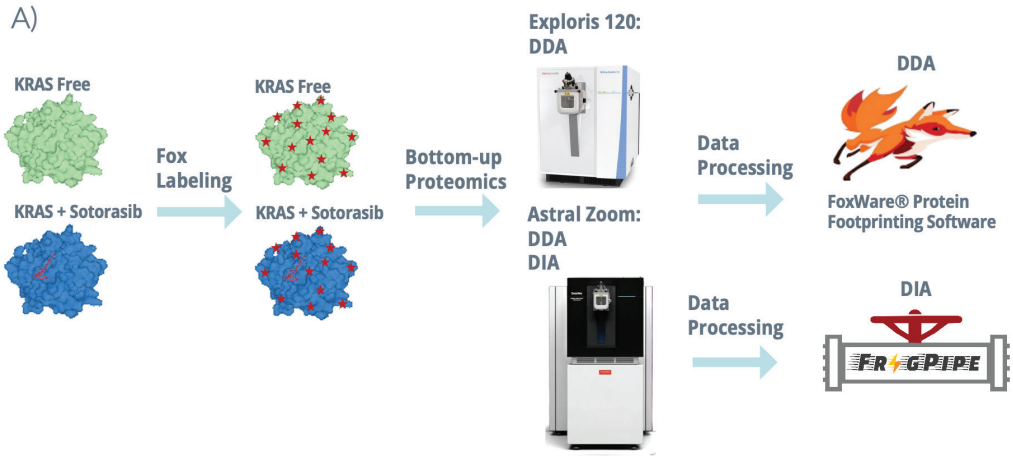

Figure 4A: HRPF Workflow with DDA and DIA MS Acquisition.

KRAS is a small GTPase that acts as a molecular switch in cell proliferation signaling; the G12C mutation, found in ~13% of non-small cell lung cancers, locks KRAS in its constitutively active GTP-bound state, driving uncontrolled tumor growth. Sotorasib (AMG 510) is a first-in-class covalent inhibitor that exploits the mutant cysteine at position 12 to irreversibly bind the Switch II pocket, trapping KRAS G12C in its inactive GDP-bound conformation. (A) Purified KRAS G12C (Free and Sotorasib-bound) was subjected to hydroxyl radical protein footprinting (HRPF) using the AutoFox system to label solvent-accessible residues with hydroxyl radicals. Labeled samples were digested and analyzed on two platforms: a Thermo Exploris 120 (DDA only) and a Thermo Astral (DDA and DIA). DDA data from both instruments were processed using FoxWare® Protein Footprinting Software. DIA data acquired on the Astral were processed using FragPipe with DIA-NN for library-free quantification, followed by custom residue-level analysis with the following filters: (i) PeptideProphet probability ≥ 0.95 and expectation ≤ 0.05, (ii) fully tryptic peptides only, (iii) single oxidation (+15.9949 Da) per peptide with no co-occurring modifications, (iv) modified residue quantified in ≥ 5 of 6 samples, and (v) percent oxidation calculated as single-ox intensity / (unmodified + all single-ox positional isomers) × 100.

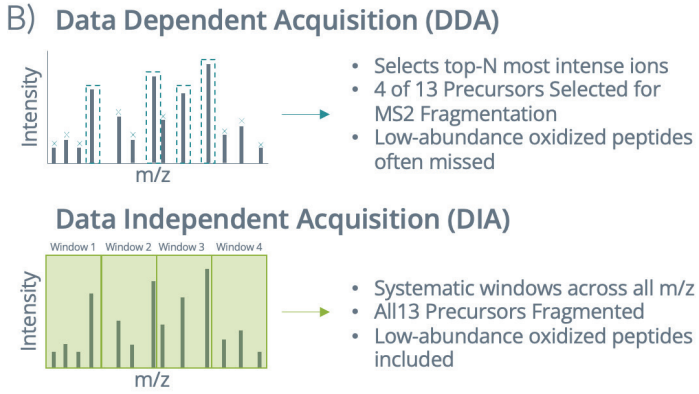

Figure 4B: DDA vs DIA MS Acquisition. *Schematic comparing DDA and DIA acquisition modes. In DDA, the mass spectrometer selects only the most intense precursor ions for MS2 fragmentation, frequently missing the low-abundance oxidized peptides critical to HRPF analysis. In DIA, systematic isolation windows tile the entire m/z range, ensuring all precursors, including low-abundance oxidized species, are fragmented in every acquisition cycle.*

DIA Acquisition on the Astral

Dramatically increases oxidized residue coverage in HRPF analysis of KRAS G12C

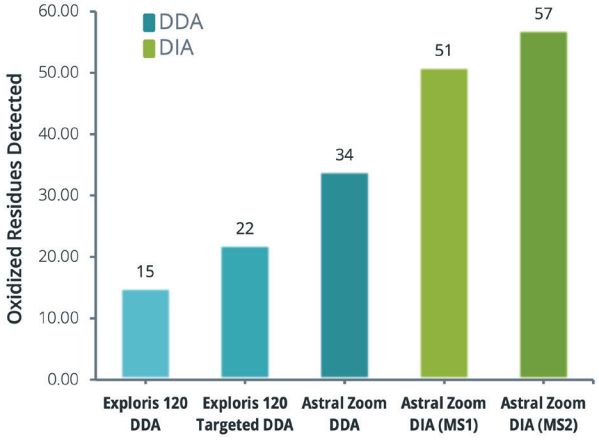

Figure 5: Number of oxidized residues across acquisition methods. *DIA acquisition detected substantially more oxidized residues than DDA across all comparisons. Standard DDA on the Exploris 120 detected 15 oxidized residues, while a targeted DDA method on the same instrument improved coverage to 22 residues by directing fragmentation toward known oxidation-susceptible peptides. Upgrading to the Astral further increased DDA detection to 34 residues, reflecting the instrument's faster scan speed and higher sensitivity. DIA acquisition on the Astral detected 51 residues using MS1 precursor-area quantification and 57 residues using MS2 fragment-level quantification — representing a 50–68% increase over Astral DDA and a nearly 4-fold improvement over standard Exploris 120 DDA. The DIA advantage is particularly relevant for HRPF, where oxidized peptides are typically present at <1–5% of their unmodified parent and are therefore disproportionately lost to stochastic sampling in DDA. All DIA results were filtered for fully tryptic peptides, single oxidation events, PeptideProphet probability ≥ 0.95, and detection in ≥ 5 of 6 replicates. DDA results were processed through FoxWare® with comparable quality filters.*

DIA Substantially Extends Oxidized Residue Coverage

Uniquely detecting 32 sites beyond DDA across the KRAS G12C sequence

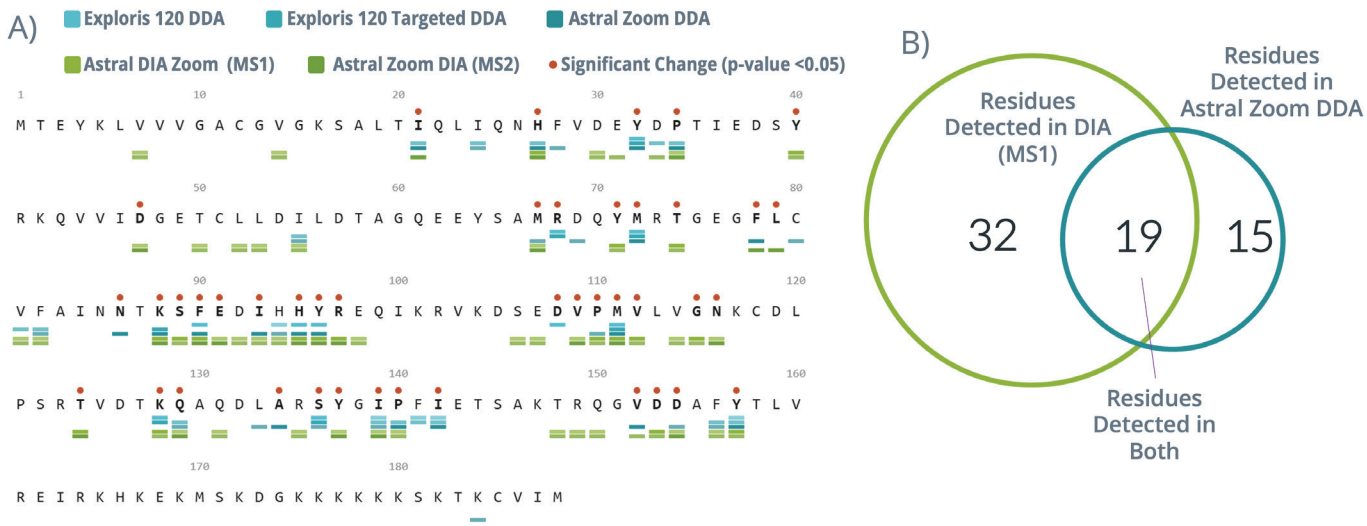

Figure 6: KRAS Oxidized Residues Coverage Map. *(A) Sequence coverage map of KRAS G12C (188 residues, 40 per line) showing oxidized residues detected by each of five acquisition methods. Identified fully tryptic peptides span the entire KRAS protein sequence from the N-terminal MTEYK motif through the C-terminal CVIM CAAX box, providing near-complete sequence coverage for footprinting analysis. Colored ticks beneath each residue indicate detection of oxidation. Orange dots above residues mark positions where at least one method detected a statistically significant change in oxidation between KRAS Free and KRAS + Sotorasib conditions ($p < 0.05$). DIA coverage is particularly dense across the Switch II region (residues 58–75), the α3 helix (residues 86–100), and the Switch II pocket floor (residues 105–116) — all regions critical to Sotorasib binding and the resulting conformational rearrangement. DDA methods show sparser coverage, with the Exploris 120 DDA limited primarily to high-abundance oxidation sites such as M67, M72, and M111. (B) Venn diagram comparing residue detection between Astral DDA and Astral DIA (MS1 quantification). Of the 51 residues detected by DIA, 19 were also detected by DDA, providing cross-platform validation at shared sites. DIA uniquely detected 32 additional residues not captured by DDA, many clustering around the Sotorasib binding interface, representing new structural information inaccessible by DDA alone. Fifteen residues were detected exclusively by DDA, likely reflecting peptides where DDA's narrow precursor isolation yields cleaner extraction than DIA's wider windows for certain co-eluting species.*

Residue-Level Percent Oxidation of KRAS G12C by DIA (MS1)

Reveals site-specific solvent accessibility changes upon Sotorasib binding

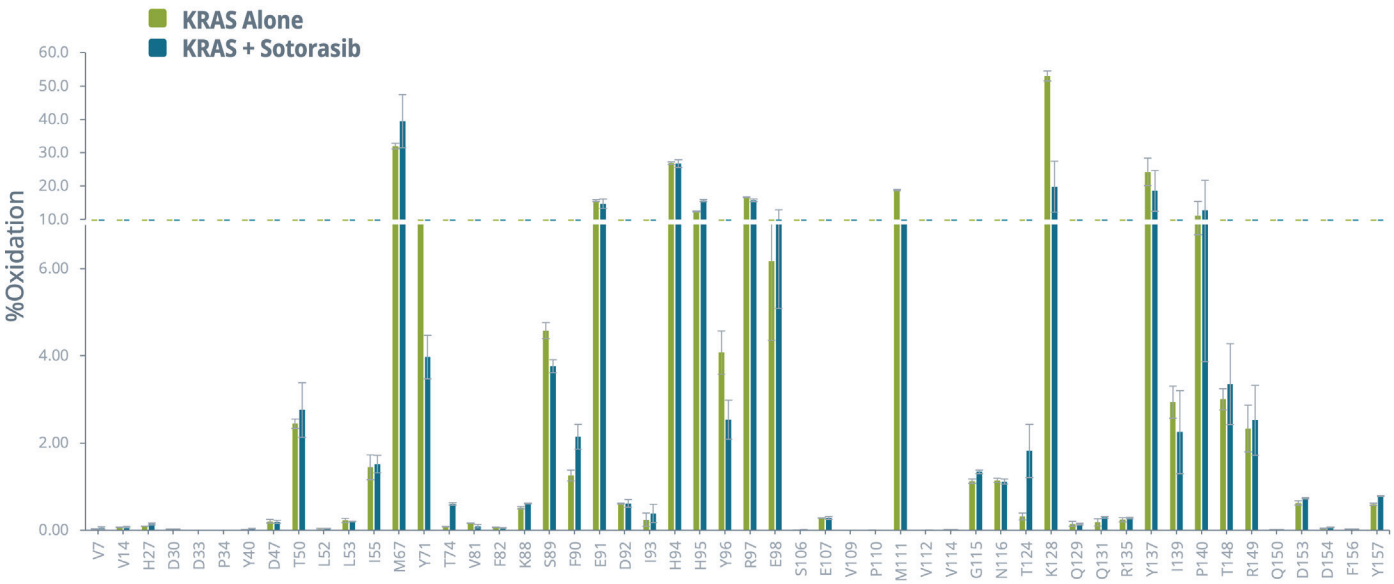

Figure 7: Residue Level Histogram. *Percent oxidation at each detected residue for KRAS Free (green) and KRAS + Sotorasib (teal), quantified by DIA acquisition on the Astral using MS1 precursor-area quantification. Bars represent the mean across three biological replicates; error bars represent standard deviation. The y-axis is split at 10% oxidation (dashed line) to resolve both highly oxidized residues and the majority of sites with lower oxidation levels. The most highly oxidized residues, M67 (~32%), H94 (~27%), M111 (~19%), Y137 (~24%), and K128 (~38–52%), reflect a combination of high intrinsic radical reactivity (Met, His, Tyr) and solvent exposure in the KRAS G12C structure. Notable changes upon Sotorasib binding include increased oxidation at M67 (32% → 39%), consistent with conformational rearrangement of the α2 helix exposing this methionine, and decreased oxidation at M111 (19% → 9%), reflecting allosteric burial of this residue as the α3-β5 loop repacks upon drug-induced opening of the Switch II pocket. H95 shows a modest increase (12% → 16%), while Y96 decreases (4% → 3%), consistent with rearrangement of the cryptic pocket formed by H95, Y96, and Q99 upon Sotorasib engagement. The majority of residues show reproducible oxidation levels across replicates (median CV < 10%), demonstrating the quantitative reliability of DIA-based HRPF at the residue level.*

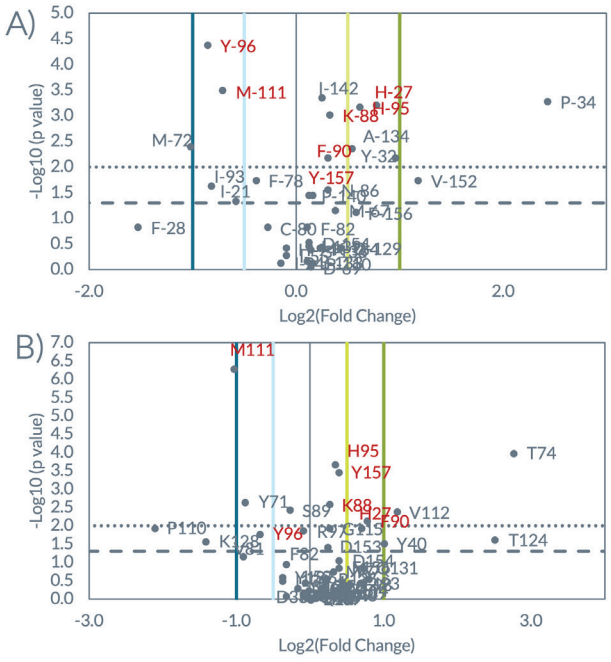

Volcano Plots Comparing KRAS G12C HRPF Results

Astral DDA and DIA (MS1) acquisition reveals concordant significant changes at key structural residues

Figure 8: Residue Level Volcano Plots. *Log2 fold change (KRAS + Sotorasib / KRAS Free) plotted against statistical significance (–log10 p-value) for (A) Astral DDA (34 residues) and (B) Astral DIA MS1 (51 residues). Vertical lines indicate fold-change thresholds; horizontal dashed line marks p = 0.05 and dotted line marks p = 0.01. Residues labeled in red were detected with a statistically significant change in oxidation (p < 0.05) in both DDA and DIA, representing the highest-confidence hits validated across both acquisition strategies. These shared significant residues include M111 (protection, consistent with allosteric burial upon Sotorasib binding), Y96 (protection, direct Switch II cryptic pocket contact), H95 and K88 (increased exposure, α3 helix rearrangement), H27 (increased exposure, Switch I), F90 (increased exposure, α3 helix), and Y157 (increased exposure, C-terminal region). DIA detected 18 significant residues*

compared to 18 for DDA, but with substantially broader overall coverage (51 vs 34 total residues), providing a more complete structural footprint. The wider spread of fold changes in the DIA plot reflects the inclusion of many low-abundance oxidation sites inaccessible to DDA, where even modest absolute changes in percent oxidation produce measurable fold changes. Both methods show strong directional agreement at shared residues, confirming that DIA faithfully reproduces the established DDA-based HRPF structural interpretation while extending it to previously undetectable sites.

Structural Mapping of Concordant DDA/DIA HRPF Changes onto the KRAS G12C–Sotorasib Complex

Reveals a coherent footprint surrounding the Switch II pocket

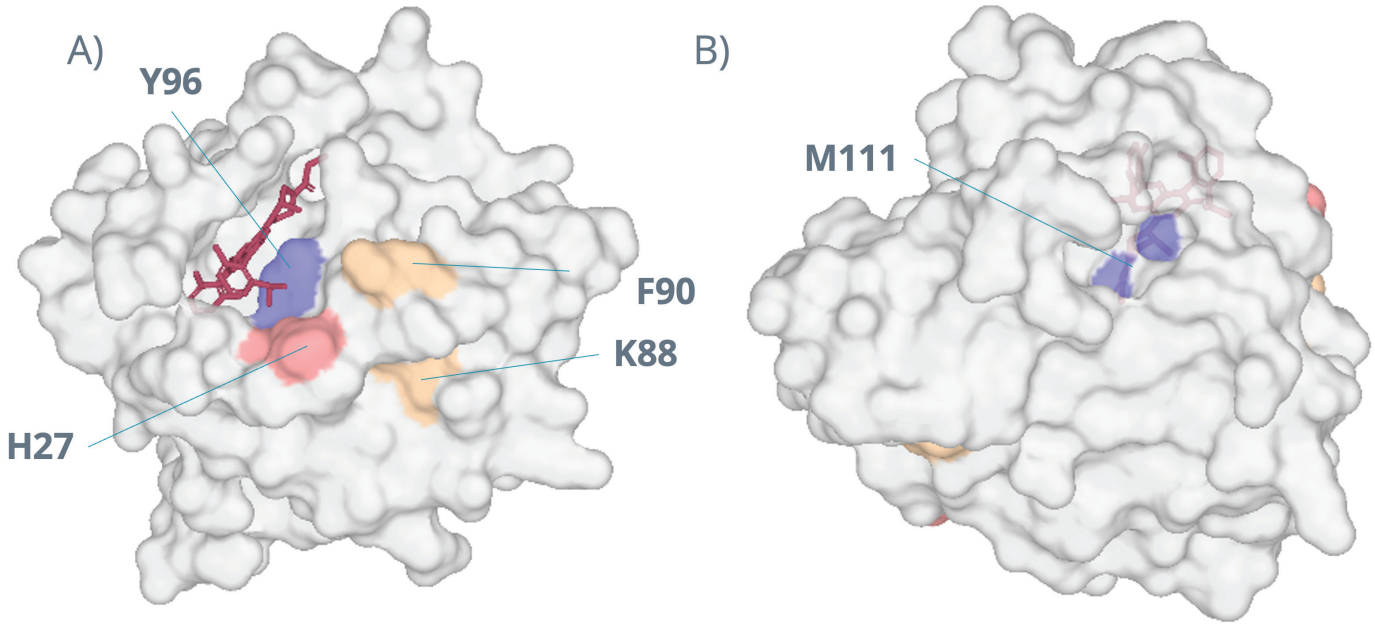

Figure 9: Switch II Pocket Decoration. *Surface representation of KRAS G12C bound to Sotorasib (dark red sticks, PDB: 6OIM) with residues showing statistically significant oxidation changes in both Astral DDA and DIA (MS1) mapped by direction and magnitude of change. Blue indicates protection (decreased solvent accessibility upon Sotorasib binding); salmon indicates increased exposure (log2 fold change between 0.5 and 1.0); wheat indicates modestly increased exposure (log2 fold change below 0.5). (A) Front view centered on the Switch II pocket. Y96, a direct contact residue within the cryptic pocket formed upon drug engagement, shows protection. H27 on Switch I shows increased exposure, reflecting destabilization of the Switch I conformation as Sotorasib locks KRAS in the inactive GDP-bound state. K88 and F90 on the α3 helix show modest increases in exposure, consistent with rearrangement of helix packing as the Switch II pocket opens to accommodate the drug. (B) Rear view revealing M111, which showed the strongest protection signal in both DDA and DIA. M111 sits in the α3-β5 loop on the opposite face of the protein from the drug-binding site, where it does not make direct contact with Sotorasib. Its protection reflects allosteric burial as this loop repacks against the α3 helix in response to the conformational rearrangement induced by drug binding.*

Conclusions

- DIA-HRPF on the Astral detected 51–57 oxidized residues on KRAS G12C — a 50–68% increase over DDA.
- DIA does not sacrifice accuracy for coverage. Residues significant in both methods showed concordant direction of change.
- The combination of HRPF labeling with DIA acquisition and FragPipe/DIA-NN processing establishes a robust, reproducible, and broadly accessible pipeline for residue-level protein structural analysis.
- AutoFox paired with DIA acquisition makes residue-level structural biology accessible without specialized expertise.
- DIA-HRPF delivers the residue-resolution structural characterization increasingly required by regulatory agencies for biosimilar comparability and higher-order structure assessment — at throughput and coverage levels compatible with development timelines.

Pairing AutoFox® labeling with DIA acquisition on the Astral unlocks residue level structural resolution at a coverage depth previously inaccessible to HRPF — delivering the kind of granular, quantitative structural characterization required for higher order structure assessment.